Measurement of fast neutron detection efficiency with ^{6}Li and ^{7}Li enriched CLYC scintillators

Measurement of fast neutron detection efficiency with ^{6}Li and ^{7}Li enriched CLYC scintillators

A Mentana[1,2]**, F Camera**[1,2]**, A Giaz**[1]**, N Blasi**[1]**, S Brambilla**[1]**, S Ceruti**[1,2]**, L Gini**[1]**, F Groppi**[1,2]**, S Manenti**[1,2]**, B Million**[1] **and S Riboldi**[1]

[1] INFN Milano, Via Celoria, 16, 20133 Milano, Italy
[2] University of Milano, Via Celoria, 16, 20133 Milano, Italy

E-mail: `alice.mentana@mi.infn.it`

Abstract. The CLYC (Cs_2LiYC_6:Ce) crystal belongs to the elpasolite scintillator family, discovered about 15 years ago. It is a very interesting material because of its good energy resolution and its capability to identify and measure gamma rays and fast/thermal neutrons. In the present work, the fast neutron detection efficiency for two different CLYC cylindrical samples has been measured. These two crystals, both with dimension (thickness x diameter) 1"x1", were respectively enriched with more than 99% of ^{7}Li (CLYC-7) and with $\sim$ 95% of ^{6}Li (CLYC-6). The presence of the ^{6}Li isotope makes the CLYC-6 ideal to detect thermal neutrons. In order to compare the two scintillators, only the detection efficiency for fast neutrons was considered, neglecting the energy region associated to thermal neutrons in both the crystals. The measurement was performed at the L.A.S.A. Laboratory of INFN and University of Milano (Italy), using a ^{241}Am-Be source.

1. Introduction

The elpasolite crystals were discovered approximately 15 years ago, and are excellent in terms of gamma and neutron detection [1]-[4]. Crystals identified as CLLB:Ce ($Cs_2LiLaBr_6$:Ce), CLLC:Ce (Cs2LiLaCl6:Ce) and CLYC:Ce belong to this new class of detectors. All these materials are suitable to identify and measure the energy of gamma rays and neutrons. The very different scintillation light decay response to different types of radiation allows them to clearly identify the incident radiation using the Pulse Shape Discrimination (PSD). The signal produced by the gamma rays contains the fast component of the scintillation light (decay time $\sim$ few ns) and the slowly decaying components channelled through the Ce^{3+} ions. The neutron signal, instead, does not have a fast component and it is characterized by a slower decay time constant [5]. Furthermore, the CLYC scintillators can detect both thermal and fast neutrons. Fast neutrons are detected using the reaction $^{35}Cl(n,p)^{35}S$ and $^{35}Cl(n,\alpha)^{32}P$ [4] where the proton or alpha particle energy is linearly related to the energy of the neutron. The thermal neutrons detection capability arises from the presence of ^{6}Li, with the reaction $^6Li(n,\alpha)t$ which has a cross-section of 940 barns.

2. The measurement

Aim of the work was to estimate the fast neutron detection efficiency of two CLYC crystals, respectively enriched with more than 99% of ^{7}Li (CLYC-7) and around 95% of ^{6}Li (CLYC-6).

The measurement was performed at L.A.S.A. Laboratory of I.N.F.N. and University of Milano in 2015, using a calibrated ^{241}Am-Be source, which generates neutrons via the following reaction:

$$^{241}Am \rightarrow \ ^{237}Np + \alpha + \gamma, \tag{1}$$

$$^{9}Be + \alpha \rightarrow \ ^{13}C^* \rightarrow \ ^{12}C^* + n. \tag{2}$$
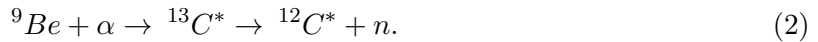
The energy spectrum of the emitted neutrons is a continuum up to around 10 MeV (see Fig. 1, [6]).

To calculate the fast neutron detection efficiency $\varepsilon_{n_{fast}}$, defined as the ratio between the fast neutron flux measured $\phi_{n_{fast}}$ and the one expected $\phi_{expected}$:

$$\varepsilon_{n_{fast}} = \frac{\phi_{n_{fast}}}{\phi_{expected}}, \tag{3}$$

one needs to count the number of fast neutrons per second interacting in the crystal ($\phi_{n_{fast}}$). The expected flux is obtained knowing the source activity A_n and the solid angles the crystal subtends, Ω ($\phi_{expected} = A_n \cdot \Omega$).

An accurate interpretation of the neutron experimental spectrum, which allows the selection of fast neutron events, is based on the detailed understanding of the neutron interaction in a CLYC scintillator.

2.1. n interaction in CLYC crystals

In CLYC-6 and CLYC-7, the fast neutron interacts with ^{35}Cl via two reactions: $^{35}Cl(n,p)^{35}S$ and $^{35}Cl(n,\alpha)^{32}P$. In CLYC-6, the ^{6}Li presence allows the detection of thermal neutron also, through $^{6}Li(n,\alpha)t$. These three reactions are characterized by three different Q-values and the emitted particles have different quenching factors f_q. Realizing that the energy measured by the crystal E_{eff}, in terms of MeVee (i.e. the scintillation light produced), is expected to be:

$$E_{eff} = (E_n + Q_{val}) \cdot f_q, \tag{4}$$

a fixed E_n value (the real neutron energy, in MeV) will correspond to three different E_{eff} values, depending on the reaction the neutron undergoes. In other words, the total experimental spectrum of neutrons from the ^{241}Am-Be source is obtained from the sum of three (or two for CLYC-7) different spectra, each one associated to a reaction, with a characteristic Q_{val} and f_q. These spectra are shown respectively in Fig. 3 for $^{35}Cl(n,p)^{35}S$, in Fig. 4 for $^{35}Cl(n,\alpha)^{32}P$ and in Fig. 2 for $^{6}Li(n,\alpha)t$ reaction. Actually, each component needs also to be weighted on its reaction cross section. The cross section curves relative to the three neutron absorption reactions are reported in Fig. 5.

To summarise, each neutron induced reaction produces a spectrum as the one of Fig. 1 shifted by the Q_{val}, scaled by the quenching factor and weighted on the cross section curves (see Fig. 6).

2.2. Fast neutron efficiency estimation

Dealing with a CLYC-7, the total ^{241}Am-Be neutron spectrum arises from the sum of the blue and red spectra of Fig. 6 (due to n interaction in ^{35}Cl). For a CLYC-6 crystal, also the green spectrum contribution of Fig. 6 has to be included (due to interaction in ^{6}Li).

Looking at Fig. 5, it is clear how the green cross section curve associated to neutron capture in ^{6}Li dominates (it is about 1000 times higher than the other curves) in the region 3.1 MeVee < E_{eff} < 3.6 MeVee, which corresponds, for these reaction, to the thermal neutron energy region. In order to be able to compare fast neutron detection efficiency for the two crystal, this region will be neglected for both.
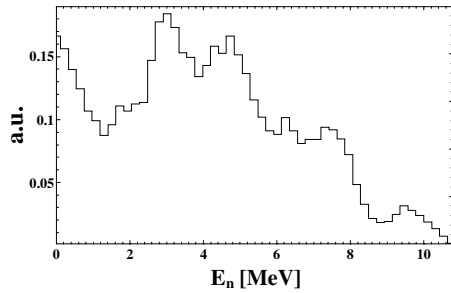
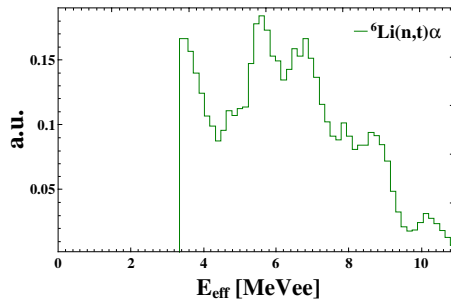**Figure 1.** Neutron spectrum of a ^{241}Am-Be source [6].

Figure 2. Neutron spectrum of a ^{241}Am-Be source as a function of the scintillation light produced, i.e. the effective energy measured E_{eff} (in MeVee), due to the reaction $^6Li(n,\alpha)t$ (only in CLYC-6).

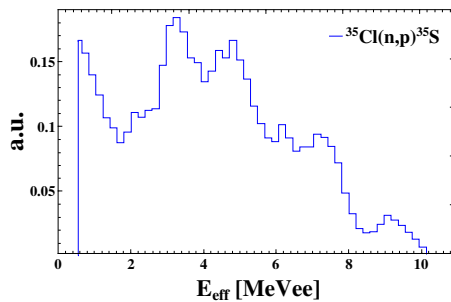**Figure 3.** Neutron spectrum of a ^{241}Am-Be source as a function of E_{eff}, due to the reaction $^{35}Cl(n,p)^{35}S$ (CLYC-6 and CLYC-7).

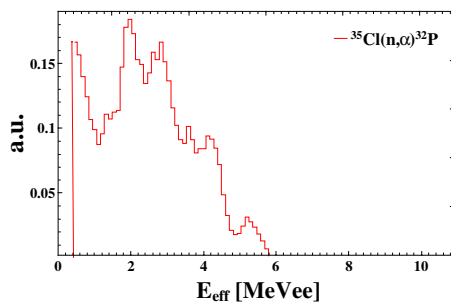**Figure 4.** Neutron spectrum of a ^{241}Am-Be source as a function of E_{eff}, due to the reaction $^{35}Cl(n,\alpha)^{32}P$ (CLYC-6 and CLYC-7).

Counting the number of neutrons in the two energy regions, 0-3.1 MeVee and 3.6-10 MeVee, the measured fast neutron flux $\phi_{n_{fast}}$ is obtained. The preliminary efficiency values, for CLYC-6 and CLYC-7, derived (eq. 3) are listed in Tab. 1.

A direct comparison between the efficiency values obtained for the two different crystals is not possible over all the energy range, due to the presence, in CLYC-6 only, of ^{6}Li. Only below 3.1 MeVee, indeed, the ^{6}Li contribution is not present. Such a contribution to the efficiency, in the
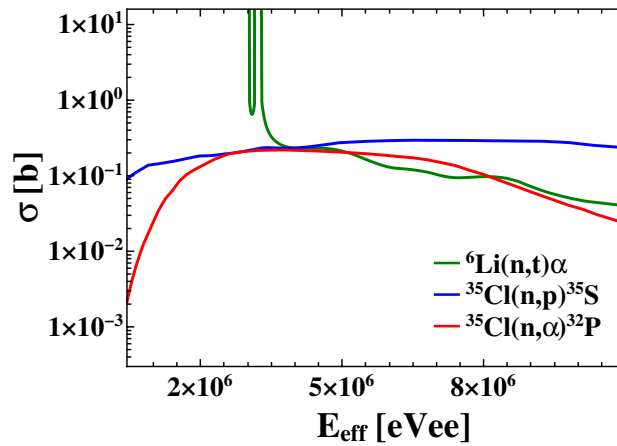
Figure 5. Comparison between the cross section curves of the three different neutron absorption reaction in terms of E_{eff}. The green curve refers to $^6Li(n,\alpha)t$ (in CLYC-6 only), the red one refers to $^{35}Cl(n,\alpha)^{32}P$ and the blue one, that dominates below 1 MeVee, refers to $^{35}Cl(n,p)^{35}S$.
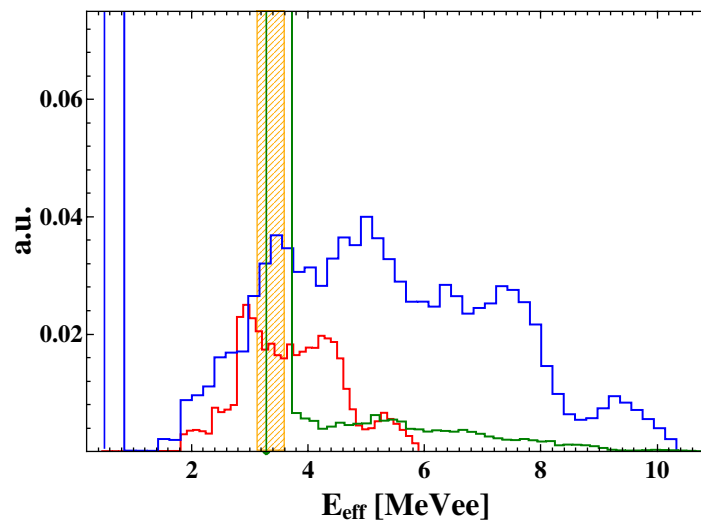

Figure 6. ^{241}Am-Be neutron predicted spectra as a function of E_{eff} weighted on the cross section for the three different neutron absorption. The blue and red spectra are referred to n interaction with ^{35}Cl, respectively $^{35}Cl(n,p)^{35}S$ and $^{35}Cl(n,\alpha)^{32}P$. The green spectrum is associated to $^6Li(n,\alpha)t$. The region between 3.1 MeVee and 3.6 MeVee (yellow rectangle) is completely dominated by the thermal neutrons peak (due to the interaction in ^{6}Li).

region over 3.6 MeVee, can be estimated taking into account the amount of Li in a Cs$_2$LiYC$_6$:Ce crystal, the isotopic abundance of ^{6}Li, the AmBe source intensity and the cross section. In this case, the ^{6}Li contribution to efficiency over 3.6 MeV is around 15%.

Table 1. The intrinsic values of fast neutron detection efficiency measured for CLYC-6 and CLYC-7.

	$\varepsilon_{n_{fast}}(\%)$
CLYC-6	(1.1 ± 0.1)
CLIC-7	(0.7 ± 0.1)

3. Conclusion

The values of intrinsic fast neutron detection efficiency has been estimated for two CLYC crystal samples, one enriched with ^{6}Li ($\sim$95%) and one with ^{7}Li (more than 99%). Such values are referred to the whole energy range, neglecting only the region associated to the interaction of thermal neutrons with ^{6}Li.

The preliminary results of this work are consistent with the ones recently published in [7] (simulation) and [8] (measurement), even though these are relative to efficiency as a function of the energy to CLYC crystal with a different relative abundance of ^{6}Li and ^{7}Li.

The forthcoming step will be to measure the fast neutron detection efficiency for the same CLYC crystals and for a larger one (2"x2" in size (thickness x diameter)) as a function of the neutron energy. For this purpose, a significant improvement in the fast neutron identification will be provided by the combined use of energy signal (the PSD technique, as in the present work) and time of flight measurement [9].

4. References

[1] Combes C M *et al* 1999 *Journal of Luminescence* B **82** pp 299-305
[2] Glodo J *et al* 2008 *IEEE Transactions on Nuclear Science* **55**,3 p 1206
[3] Glodo J *et al* 2011 *IEEE Transactions on Nuclear Science* **58**,1 p 333
[4] Smith B *et al* 2013 *IEEE Transactions on Nuclear Science* **60**,2 p 855
[5] http://rmdinc.com/about-us/dynasil-corporate-profile/
[6] Usha Pujala *et al* 2011 *Radiation Protection and Envirroment* **34** pp 262-266
[7] D'Olympia N *et al* 2014 *Nuclear Instrumental and Methods in Physisce Research A* **763** pp 433-441
[8] Smith B *et al* 2015 *Nuclear Instrumental and Methods in Physisce Research A* **784** pp 162-167
[9] Giaz A *et al* 2016 *Nuclear Instrumental and Methods in Physisce Research A* **825** p 51